Journal of Hazardous Materials 185 (2011) 639–646

Contents lists available at ScienceDirect

Journal of Hazardous Materials

journal homepage: www.elsevier.com/locate/jhazmat

Sorption and desorption of pentachlorophenol to black carbon of three different origins

Ling Luo, Liping Lou*, Xinyi Cui, Binbin Wu, Jiaai Hou, Bei Xun, Xinhua Xu, Yingxu Chen

Department of Environmental Engineering, Zhejiang University, Hangzhou 310029, People's Republic of China

ARTICLE INFO

Article history:
Received 1 April 2010
Received in revised form
10 September 2010
Accepted 21 September 2010
Available online 25 September 2010

Keywords:
Black carbon (BC)
Pentachlorophenol (PCP)
Irreversible sorption
Hysteresis

ABSTRACT

Rice straw charcoal, soot and fly ash (collectively termed "black carbon" or BC), which were found to widely exist in the environment and exhibit strong sorption of many organic compounds, were prepared for this study, and recorded as RC, SC, and FC, respectively. The characterization, sorption isotherm, and the effect of pH (from 3.0 to 9.0) on sorption capacity of each BC were investigated. It is demonstrated that RC possessed the largest surface area (234.9 m^2/g), the highest porosity (0.4392 mL/g), and the largest amount of functional groups (2.995 mmol/g) of all. All the Freundlich, Langmuir and Dual-mode model can fit the sorption data of each BC well. The pH value could apparently affect the sorption capacity of pentachlorophenol (PCP) to BCs, which reached maximum value at pH 4.0. Furthermore, in order to validate the effect of pH on desorption capacity, we designed sorption–desorption cycle experiments at pH 9.0 and then pH 7.0, and found that the effect of pH on irreversible sorption and hysteresis effects were significant. As pH value decreasing from 9.0 to 7.0, the irreversible sorption capacities for RC, FC, and SC increased, and the desorption hysteresis index (H) values of PCP increased approximately 3 times for each BC.

1. Introduction

There is an accumulating body of evidence that suggests black carbon (BC), generated from incomplete combustion of biomass and fossil fuels, could act as supersorbent for contaminants in soils or sediments [1–5]. Pure BCs could adsorb up to 10–1000 times stronger than other types of organic carbon (OC) [6,7]. BCs have demonstrated high and nonlinear sorption of organic compounds [6], and were responsible for more than half of the total sorption in the nanogram per liter range [8]. As sorption is one of the key factors regulating the bioavailability and the toxicity of organic contaminants in soils or sediments, a better understanding of the sorption behavior and mechanisms of organic pollutants to BC is crucial to assess the ecological risks of these chemicals.

Many studies have been conducted about the sorption of hydrophobic organic compounds (HOCs) by BC from a single source, such as crop-ash, fly ash, or soot [9–11]. It is widely agreed that the properties and the sorption behavior of BC will vary, depending on the type of the raw materials, as well as the combustion conditions [12]. Jonker and Koelmans [13] investigated the sorption of PAHs and PCBs on several BCs, they found that fly ash and coal soot always had the lowest sorption values whereas activated carbon was shown to have the highest sorption for all compounds measured, and differences as large as 4 log units were often observed between these two extremes. Nguyen and Ball [14] investigated the sorption of HOCs employing four kinds of soot (i.e., hexane soot, ozonated hexane soot, diesel soot SRM 2975, and diesel soot SRM 1650b) with various properties, and found that samples with higher O/C ratio or higher content of extractable antigenic organic chemicals showed less sorption. However, studies which compared the sorption behavior among different kinds of BC, or related sorption with intrinsic properties of different BC particles, are still scarce.

Pentachlorophenol (PCP) has been used as an industrial antiseptic and biocide for many decades since the 1960s. Due to its proven carcinogenicity, toxicity, and ubiquity, PCP has been designated as a "priority toxic pollutant" by the United States Environmental Protection Agency (EPA) [15]. In China, PCP was produced and used extensively from 1960s until 2000, and generated a large amount of residues in the environment even now [11]. Duan et al. [16] have shown that the concentrations of PCP were 3.61–2010 ng/L in river water and seawater in China. On the other hand, previous studies about the sorption on BC mainly focused on only several classes of chemicals, such as polycyclic aromatic hydrocarbons (PAHs), polychlorinated biphenyls (PCBs), polybrominated diphenyl ethers (PBDEs), chlorobenzene, or some pesticides, but the sorption of PCP by BC has received relatively little attention. Moreover, there is little information about the effect of pH on the sorption of PCP by different kind of BC, or the PCP sorption hysteresis by different BC.

* Corresponding author. Tel.: +86 571 86971502; fax: +86 571 86971360.
E-mail address: loulp@zju.edu.cn (L. Lou).

0304-3894/$ – see front matter © 2010 Elsevier B.V. All rights reserved.
doi:10.1016/j.jhazmat.2010.09.066

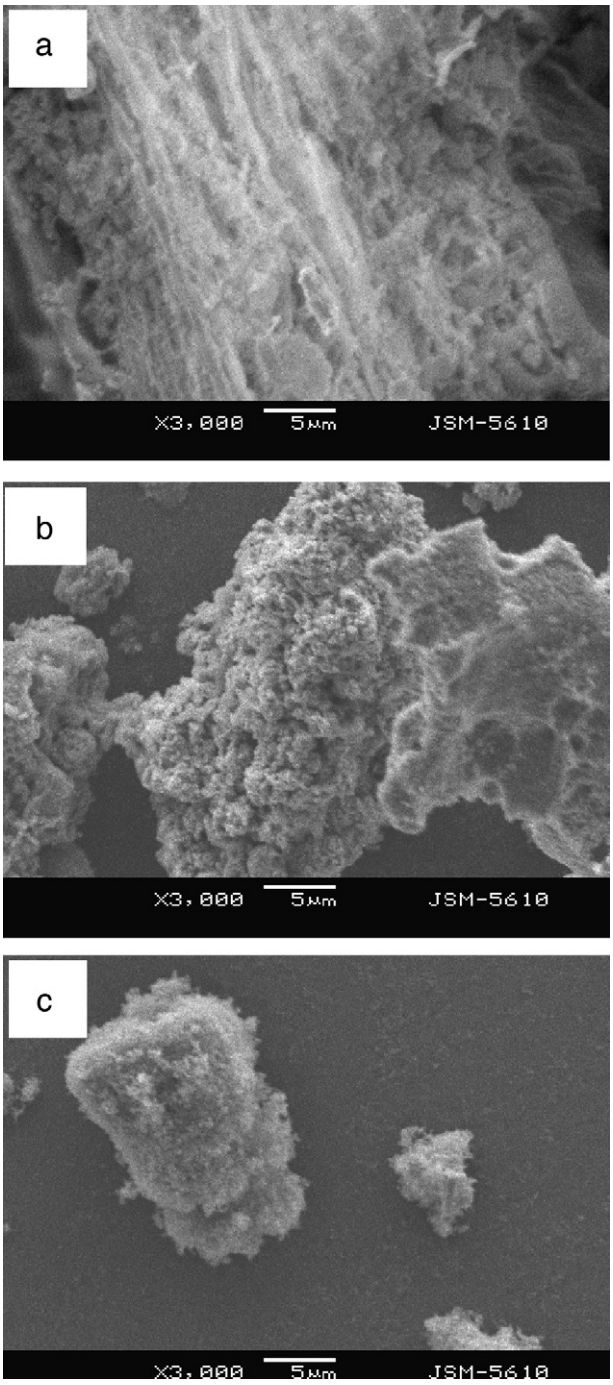

Fig. 1. Scanning electron microscopy images of black carbons with a magnification of ×3000: (a) RC; (b) FC; and (c) SC.

In this study, rice straw charcoal, fly ash, and soot were selected as representatives of BC particles with different characteristics. Based on the information about surface properties among different BCs, sorption properties and effect of pH on the sorption capacity of PCP to each BC were studied. Moreover, cycles of sorption–desorption tests at pH 9.0 and then pH 7.0 were conducted to investigate irreversible sorption of PCP to BCs influenced by pH.

2. Experimental

2.1. Chemicals and materials

PCP, with a purity of >98%, was purchased from Sigma–Aldrich (China). It is a highly chlorinated HOC and a weak acid with a pK_a of 4.75, and its aqueous solubility (S_W) at 25 °C usually ranges from 25 to 30 μg/mL [9].

Rice straw charcoal, fly ash, and soot, were used as precursors of BC. Dry rice straw was cut into small pieces (<20 mm) and oven-dried at 105 °C. The rice straw was placed in a ceramic pot, covered with a fitting lid, and pyrolyzed under the oxygen-limited conditions for 3 h at 600 °C [1]. The fly ash produced during the combustion of coal (at 1400 °C) was collected on electrostatic filters of Hangzhou thermoelectric plant, Zhejiang province, China. Soot was purchased from Degussa Company, Germany. These samples were treated to get purified BC using a similar method from some previous papers [1,10,12] with slight modifications. Briefly, each BC sample (10 g) was treated in 200 mL of 2 M HCl for 24 h at 25 °C and centrifuged at 4800 rpm for 20 min to remove the supernatants, and this procedure was then repeated four times. Subsequently, the same procedure was performed except that 1 M:1 M HCl–HF solution was used instead of 2 M HCl. The treated samples were then thoroughly washed with distilled water five times to remove residual acids, Si, and soluble salts. The treated rice straw charcoal, fly ash, and soot were oven-dried overnight at 105 °C, and recorded as RC, FC, and SC, respectively.

2.2. Characteristics of RC, FC, and SC

The elemental composition (C, H, N) of the treated RC, FC, and SC were determined by an Element Analyzer (EA 1110, USA). The surface area and pore volume of BC samples were measured by a 100CX surface area analyzer (Coulter Omnisorp, USA). The BET (Brunauer–Emmerr–Teller) equation was used to calculate the surface area of BCs and the total pore volume (i.e., sum of micro- and mesopore volume) was defined as the volume of nitrogen adsorbed at the $P/P_o = 0.981$ [17]. The structure and morphology of each BC sample were examined using a scanning electron microscopy (SEM, JSM-5610LV, Jeol, Japan) at ambient temperature and 10.0 kV.

The surface acidity and basicity were determined using the Boehm's titration method [1,11]. Each BC (0.500 g) was accurately weighed and reacted with 25 mL of 0.1 M Na_2CO_3, $NaHCO_3$, NaOH, $NaOC_2H_5$ or HCl solution in 50-mL conical flasks for 48 h. The back-titration was carried out using 0.1 M HCl or NaOH solution to neutralize the excess acid or base. Surface acidity and basicity were calculated on the basis of the assumption that $NaHCO_3$ neutralizes carboxyl groups only, Na_2CO_3 neutralizes carboxyl and lactonic groups, NaOH neutralizes carboxyl, lactonic and phenolic groups, $NaOC_2H_5$ neutralizes carboxyl, lactonic, phenolic and quinonyl groups, and HCl neutralizes all basic groups. Furthermore, in order to validate the presence of surface functional group, the FTIR (Fourier transform infrared spectroscopy) spectra of BC samples were recorded using a Nicolet Impact 410 FTIR spectrometer (Nicolet Instrument Corporation) with 4 cm^{-1} resolution and 64 scans between wavenumbers of 400 and 4000 cm^{-1}.

2.3. Sorption experiments

In this study, PCP was dissolved in methanol to form a 250 mg/L stock solution. Before use, the stock solution was diluted into a set of concentrations ranging from 0.1 to 20 mg/L with an electrolyte matrix containing 1 mM $CaCl_2$, 1 mM $MgCl_2$, and 0.5 mM $Na_2B_4O_7{\cdot}10H_2O$, with 200 μg/mL NaN_3, which was added to inhibit aerobic biodegradation [18]. All sorption experiments were con-

ducted in triplicates in 50-mL glass centrifuge vials. The RC, FC, and SC to water ratio (W/V) were adjusted to achieve 30–70% of the total sorbed solute. After aliquots of RC, FC, and SC were added respectively, each vial received 30 mL background electrolyte solution containing various concentrations of PCP. The vials were shaken at 200 rpm on a horizontal shaker at 25 ± 1 °C for 24 h in the dark. Preliminary tests indicated that 24 h was sufficient to reach the apparent equilibrium. After the establishment of sorption equilibrium, sorbents and aqueous phases were separated by centrifugation at 3000 rpm for 20 min. An aliquot of 1 mL of the supernatant liquid was filtered through a 0.45 μm Millipore membrane. Then, the PCP concentrations were analyzed using high performance liquid chromatography (HPLC). Blanks loaded with PCP solution without BC were also run to assess losses of solutes to reactor components in the sorption process.

PCP concentrations in the initial and the equilibrated supernatants were analyzed using an Agilent 1100 series HPLC with a diode array UV detector and a C_{18} reversed-phase column (ODS, 5 μm, 2.1 mm × 250 mm). Methanol and 1% acetic acid (90:10, v/v) were used as a mobile phase at a flow rate of 1.0 mL/min, and the injection volume was 20 μL. The UV wavelength for detection of PCP was set at signal wavelength of 220 nm with a 20-nm bandwidth, and a reference wavelength of 300 nm with a 50-nm bandwidth. The compound concentrations were quantified with an external standard method [18].

2.4. Effect of pH on sorption experiments

Due to the special acid–base ionogenic behavior of PCP and the different properties of RC, FC, and SC, it is important to investigate the PCP sorption on each BC as a function of pH values. The pH of PCP-spiked level background electrolyte solution (mg/L) was adjusted to the range of 3.0 to 9.0, respectively with 0.1 mol/L HCl or NaOH solution. After that, sorption equilibrium experiments were conducted in the same way as described above, in triplicate, and blanks were essential. In addition, we also determined the pH value after sorption completed.

2.5. Sorption–desorption cycle experiments

The experiments consisted of repeated cycles of sorption and desorption. A cycle of sorption and desorption consisted of sorption followed by several successive desorption steps. Sorption was performed in triplicate in 50-mL glass vials as described previously, and the solid-to-water ratio varied for different BC samples. After the sorption period, desorption was conducted by withdrawing 90% the supernatant and replenishing the samples with fresh PCP-free background electrolyte solution (the actual amounts were determined by weight). The vials were sealed, shaken for 24 h at 200 rpm at 25 ± 1 °C in the dark, and then centrifuged at 3000 rpm for 20 min. The supernatant was analyzed for solution-phase PCP concentration by HPLC. After the successive desorption steps, the solution was decanted and wet BC was left in the bottle. 30 mL of PCP solution was added to the vial to carry out another cycle of sorption–desorption experiments. To consider the effect of pH value on PCP sorption, the pH value of PCP solution was adjusted to 9.0 in cycles 1 and 2, and to 7.0 in cycles 3 and 4. The pH of the electrolyte solution was in accordance with that in the PCP solution. Blanks filling PCP solution without BC were also run to assess losses of solutes due to sorption on glass tubes and evaporation during the sorption–desorption tests.

2.6. Data analysis

Three different models were used to fit the adsorption data. The Freundlich model (FM), which used commonly for quantifying HOC sorption equilibria for soils and sediments, has the following form

$$q_e = K_f C_e^N \quad (1)$$

where K_f [(mg/kg)/(mg/L)^n] and N are respectively the Freundlich model capacity factor and the isotherm linearity parameter, an indicator of site energy heterogeneity [9]. The Langmuir model (LM) describing such site-limiting sorption equilibrium has the following form

$$q_e = \frac{Q_{\max} C_e}{K_L + C_e} \quad (2)$$

where $Q_{\max}$ is the maximal sorption capacity and K_L is a solute–surface interaction energy-related parameter [19]. Sorption isotherms were also fit to the Dual-mode model (DMM), which includes solid-phase dissolution (partitioning) described by a linear term and hole-filling described by a Langmuir term. The DMM is given by

$$q_e = K_D C_e + \frac{Q_{\max,L} C_e}{K_{L,D} + C_e} \quad (3)$$

where K_D is the dissolution domain partition coefficient, and $Q_{\max,L}$ and $K_{L,D}$ are the capacity and affinity coefficient, respectively, of the hole-filling domain [19]. The $Q_{\max,L}/(K_D,K_{L,D})$ value represents the intrinsic affinity of solute for the hole-filling domain relative to the dissolution domain given infinite dilution [9].

Based on the Gibbs equation, the standard molar Gibbs free energy change is calculated as

$$\Delta G^0 = -RT \ln K_{OC} \quad (4)$$

where R is the universal gas constant (J/(mol K)), T is absolute temperature (K), and $K_{OC} = (q_e/C_e)/f_{oc}$ [9].

The sorption–desorption apparent hysteresis index (H) was determined by the equation:

$$H = \frac{N}{N_d} \quad (5)$$

where N and N_d are the Freundlich exponents calculated from the sorption and desorption isotherms, respectively [20].

3. Results and discussion

3.1. Characterization of RC, FC, and SC

The elemental composition, surface area and pore volume of BCs are listed in Table 1. The elemental analysis showed that SC had the highest content of C (91.46), but RC exhibited the higher H/C ratio (0.032) (increasing with less carbonized [7]), surface area (234.9 m^2/g) and porosity (0.4392 mg/L) than FC and SC (Fig. 1). The SEM images revealed that SC particle was a uniform ball with a diameter of less than 1 micron, and it was smaller and more regular than RC and FC. The structures RC derived apparently from the reedy fibers of rice straw.

The total acidity and basicity of RC, FC, and SC from the Bohem titration are shown in Table 2. It is evident that there were no basic groups in each BC due to the acid demineralization in the removal of inorganic salts, but a large amount of acidic functional groups, especially the carboxylic acid. By comparison, RC had the largest content of surface acidity functional groups (2.995 mmol/g), and FC possessed the smallest content (0.984 mmol/g). Furthermore, to obtain the surface density of groups for a better correlation with PCP sorption–desorption data in the later discussion, the total acidity was normalized to the surface area of corresponding BC. In Table 2, RC had the lowest density of groups (7.68/nm^2), while FC possessed the highest density of groups (28.21/nm^2).

In addition, the BC surface properties as affected by the raw materials and combustion conditions were further illustrated by

Table 1
Elemental compositions, atomic ratios, surface area, and pore volume of RC, FC, and SC.

BC	Elemental composition (%)			Atomic ratio		Surface area (m^2/g)	Mesopore	
	C	H	N	H/C	N/C		Porosity (mL/g)	Average pore size (nm)
RC	37.87	1.21	0.33	0.032	0.009	234.9	0.4392	64.3
FC	29.68	0.26	0	0.009	0.000	21.0	0.0387	20.53
SC	91.46	0.97	0	0.011	0.000	50.5	0.170	19.87

Table 2
Boehm titration results and density of surface functional groups (mmol/g).

BC	Boehm titration (mmol/g)							Density of groups (group/nm^2)
	Carboxyl	Lactone	Phenolic	Quinonyl	Acidic	Basic	All	
RC	2.418	0.070	0.350	0.158	2.995	0.000	2.995	7.68
FC	0.494	0.000	0.000	0.490	0.984	0.000	0.984	28.21
SC	1.014	0.240	0.161	0.016	1.431	0.000	1.431	17.06

the FTIR data in Fig. 2. FTIR spectra of BCs were characterized by four principal bands at wavenumbers of 3435 cm^{-1} (OH), 1620 cm^{-1} (C=O), 1090 cm^{-1} (C–O), 795 cm^{-1} (CH_2) [1,21]. The peaks' number and intensity of FTIR spectra of various BC was in the order of RC > FC > SC.

As a result, it can be deduced scientificly that the surface characteristics of BCs, produced from different materials and conditions, differed distinctly in the formation of surface area, pore volume, elemental composition, and functional group, etc.

3.2. Sorption isotherms

Sorption data of PCP to RC, FC, and SC are plotted in Fig. 3, while the parameters of RC, FC, and SC fitted by FM, LM and DMM are listed in Table 3. The FM described all the sorption isotherm data well with R^2 ranging from 0.924 to 0.986, and the N values (decreasing with increasing nonlinearity) were 0.32, 0.37, and 0.42 for RC, FC, and SC, respectively, indicating that all the isotherm curves were nonlinear. Fitting of the sorption data with LM revealed that RC possessed the highest Q_{max} value (25.14 mg/g), SC and FC were 10.91 and 2.96 mg/g, respectively. The DMM model gave a good fit to sorption data (R^2 ranging from 0.927 to 0.993), and provided the $Q_{max,L}/(K_D K_{L,D})$ values. It is found that SC had the highest $Q_{max,L}/(K_D K_{L,D})$ value (74.54) of all, and might have the dominating sorption mechanism of adsorption (hole-filling). Although all the models can describe the sorption data well, the Freundlich model was only applied to the further study for the sake of obtaining the sorption–desorption hysteresis index (H) value of PCP to BCs.

There are many mechanisms to explain the sorptive observations: surface coverage, multilayer adsorption, condensation in capillary pores, and absorption into the polymeric matrix [19]. The hole-filling adsorption was considered as the important contribution to sorption capacity of HOCs at relatively low and high concentrations [4,9,20,22].

In our research, the obtained values of ΔG^0 were all negative and much less than 40 kJ/mol, which can be regarded as the critical values for the estimation of the dominant sorption mechanisms, under which the sorption of PCP on BCs might occur dominantly in adsorption (hole-filling) [9]. Standardization of K_{OC} by dividing the surface area of each BC was quite similar, that is to say the surface adsorption was one of the sorption mechanism [6]. It is also worth mentioning that the sorption capacity of BC sample seems to be positively related to the surface area and porosity.

As stated previously, it is hard to infer which was the main sorption mechanism between hole-filling and surface adsorption, or both of them were sorption mechanisms in the research. Therefore, further researches on sorption mechanisms of HOCs to BCs will still be needed.

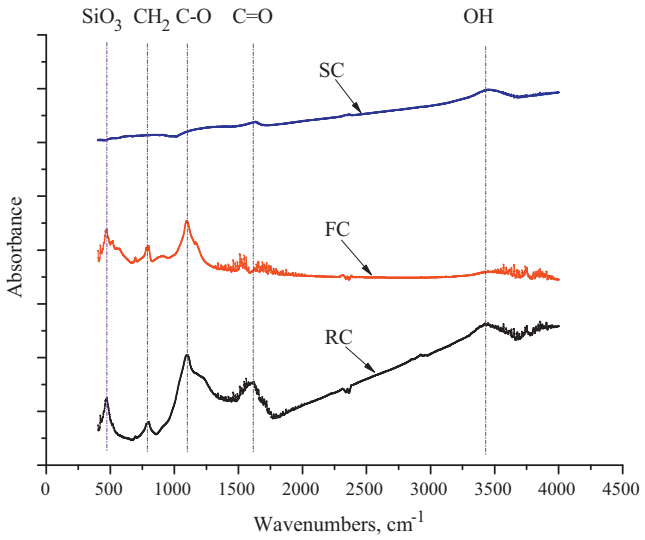

Fig. 2. FTIR spectra of RC, FC, and SC.

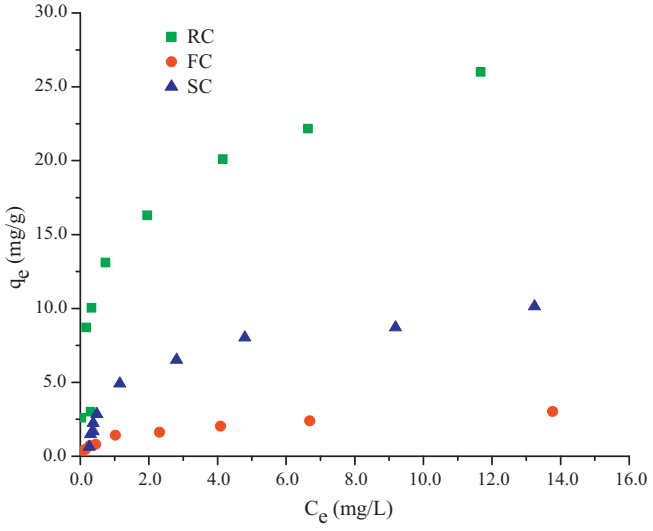

Fig. 3. Sorption isotherms of PCP to RC, FC, and SC. q_e is the amount of PCP sorbed per mass of soils, C_e is the equilibrium PCP concentration. The symbols denote experimental data points (pH 7.0).

Table 3
FM, LM, and DMM sorption parameters for sorption of PCP to RC, FC, and SC (pH 7.0).

Sorption model		RC	FC	SC
FM	K_f	12.29 ± 0.99	1.18 ± 0.05	3.63 ± 0.36
	N	0.32 ± 0.04	0.37 ± 0.02	0.42 ± 0.05
	R^2	0.912	0.984	0.929
LM	Q_{max}	25.14 ± 2.20	2.96 ± 0.23	10.91 ± 0.49
	K_L	0.74 ± 0.24	1.30 ± 0.34	1.70 ± 0.24
	R^2	0.889	0.941	0.981
DMM	K_D	0.72 ± 0.46	0.09 ± 0.01	0.09 ± 0.11
	$Q_{max,L}$	18.30 ± 4.16	1.81 ± 0.14	9.66 ± 1.63
	$K_{L,D}$	0.39 ± 0.22	0.47 ± 0.09	1.44 ± 0.40
	R^2	0.927	0.993	0.984
	$Q_{max,L}/(K_D K_{L,D})$	65.17	42.17	74.54
ΔG^0 (kJ/mol)		−19.10	−13.37	−16.40

FM: Freudlich model, $q_e = K_f C_e^N$; LM: Languir model, $q_e = Q_{max} C_e/(K_L + C_e)$; DMM: Dual-mode model, $q_e = K_D C_e + (Q_{max,L} C_e/(K_{L,D} + C_e))$.

3.3. Effect of pH on sorption

The sorption curves of PCP on RC, FC, and SC at various pH values are shown in Fig. 4. All curves demonstrated a similar trend, the maximum sorption capacity was reached at pH 4.0, while decreasing gradually with increasing pH values. During the sorption experiments, we determined the pH value of solution before and after experiments, and found that the pH of sorption and desorption systems almost remained unchanged.

The pH effect may be connected to two aspects, the surface properties of BC and the speciation of HOCs. The former is characterized primarily by the surface functionality. Chun et al. [1] reported the hydrophilic groups of BC (e.g., —OH and —COOH) could act as water adsorption sites, and in the presence of water, effectively obstruct the surface accessible otherwise to HOCs [23]. Depending on pH, the protonation and deprotonation of functional groups result in a different net charge on the BC surfaces. In the acidic condition (from pH 3.0 to pH 7.0), the surface functional groups of each BC have already become acidic radicals, which had less electricity as they hardly dissociated, and possessed weak hydrophilicity, and had a tendency to make macromolecule crimpled [21]; however, in alkaline environment (from pH 7.0 to pH 9.0), the acidic groups of BCs reacted with hydroxyl, so some of the sorption capacity, which caused by the surface functional groups, accordingly decreased.

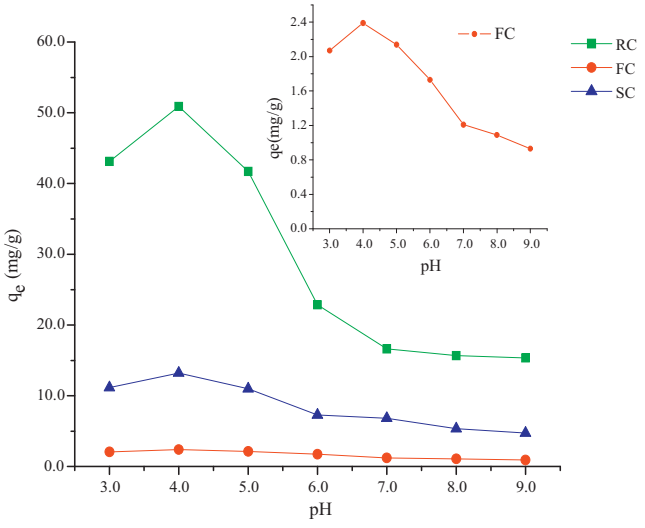

Fig. 4. Sorption capacity of PCP sorbed on RC, FC, and SC at different pH value ranging from 3.0 to 9.0.

On the other hand, protonation or deprotonation of a dissociable HOC is similarly determined by pH. PCP is a hydrophobic weak organic acid ($pK_a = 4.75$) and exists as either a neutral or an ionized species—PCP^n and PCP^-, respectively. The proportion of PCP^n and PCP^- changed with the pH values, e.g., PCP^n accounted for more than 99% of all the PCP at pH 4.0, and only 5% when pH was above 6.0. Moreover, the neutral form of PCP was strongly hydrophobic and highly sorptive, and affinity with solid particles of PCP became the highest at pH 4.0, approaching the value of pK_a [24–26]. It is why the sorption capacity increased from pH 3.0 to pH 4.0, but decreased when the pH value increased from 4.0 to 9.0 in the current study.

3.4. Sorption–desorption cycle isotherms

The desorption isotherms for RC, FC, and SC are shown in Fig. 5. All the desorption data could be well described by the Freundlich model, with R^2 ranging from 0.860 to 0.996, and every desorption isotherm was nonlinear with N value less than 0.281. When compared with adsorption isotherms, all the BC particles exhibited sorption–desorption hysteresis.

For the convenience of comparing the irreversibility of sorption–desorption, the Hysteresis Index (H) was applied. It is evident from the information presented in Table 4 that the calculated H values for all BCs were greater than zero [27,28], indicated the occurrence of sorption–desorption hysteresis for RC, FC, and SC. In the sorption–desorption cycles, the H values of PCP in each BC followed the order: FC > RC > SC. In cycles 1 and 2 (pH 9.0), the H values of RC, FC, and SC were 1.69, 1.75, 0.67 and 2.25, 2.10, 0.80 respectively; in cycles 3 and 4 (pH 7.0), the H values of RC, FC, and SC were 5.33, 6.17, 2.21 and 4.57, 6.17, 2.10, respectively. It is obvious that

Table 4
Multiple sorption–desorption isotherm parameters fitted by Freundlich model and sorption–desorption hysteresis index.

BC		N	N_d	R^2	H
RC	Cycle 1	0.27 ± 0.03	0.16 ± 0.01	0.939	1.69
	Cycle 2	0.27 ± 0.03	0.12 ± 0.02	0.915	2.25
	Cycle 3	0.32 ± 0.04	0.06 ± 0.01	0.952	5.33
	Cycle 4	0.32 ± 0.04	0.07 ± 0.01	0.943	4.57
FC	Cycle 1	0.21 ± 0.03	0.12 ± 0.01	0.951	1.75
	Cycle 2	0.21 ± 0.03	0.11 ± 0.02	0.867	2.10
	Cycle 3	0.37 ± 0.02	0.06 ± 0.01	0.877	6.17
	Cycle 4	0.37 ± 0.02	0.06 ± 0.01	0.974	6.17
SC	Cycle 1	0.20 ± 0.05	0.30 ± 0.04	0.891	0.67
	Cycle 2	0.20 ± 0.05	0.25 ± 0.05	0.825	0.80
	Cycle 3	0.42 ± 0.05	0.19 ± 0.03	0.896	2.21
	Cycle 4	0.42 ± 0.05	0.20 ± 0.01	0.996	2.10

N and N_d: parameters fitted by Freundlich sorption model; H: Sorption–desorption hysteresis index, $H = N/N_d$.

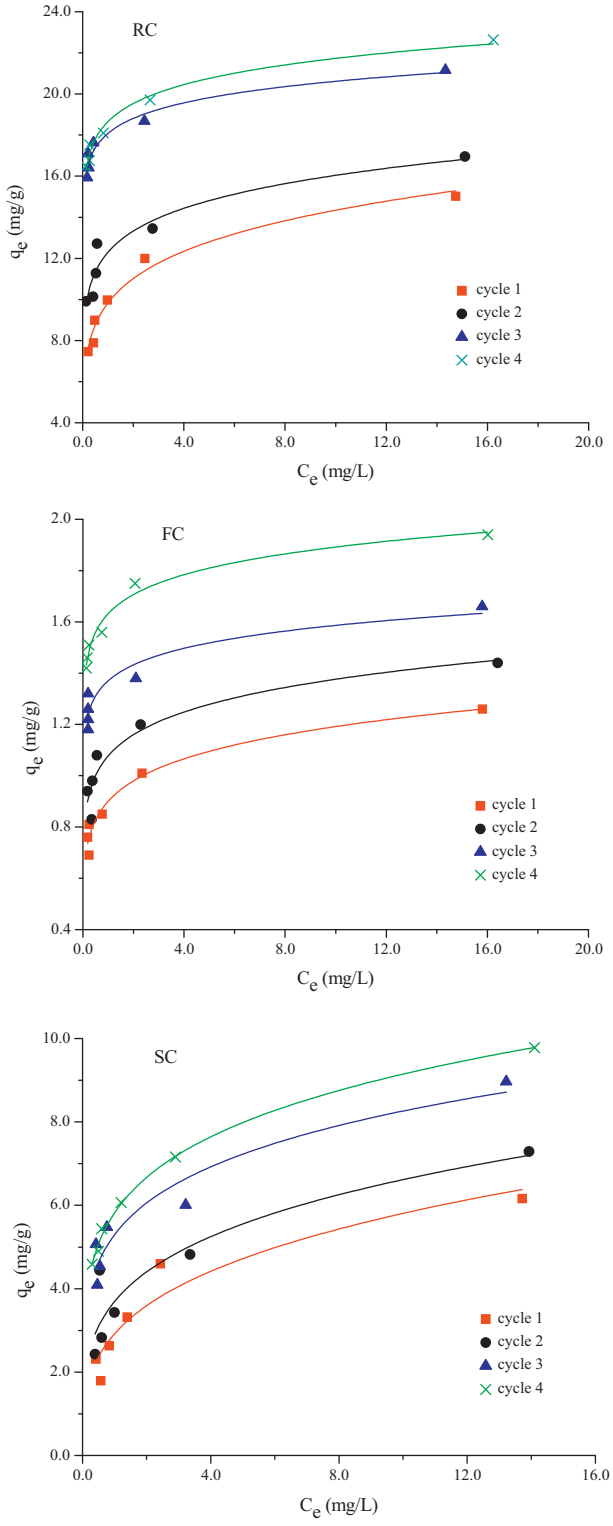

Fig. 5. The Freundlich model fitted of desorption isotherm data for RC, FC, SC. Solid lines represent model fittings, q_e is the amount of PCP sorbed per amount of sediment, and C_e is the equilibrium PCP concentration. The symbols denote experimental data points.

the H values increased along with pH values descending from 9.0 to 7.0.

The available form of PCP at pH 9.0, basically PCP^-, accounted for more than 95% of the total PCP, was similar to pH 7.0. In addition, the surface properties and organic configurations of each BC at pH 9.0 were obvious different than pH 7.0 because the functional groups of BCs (e.g., —OH and —COOH) may be largely dissociated in the stronger basic condition. In this case, PCP couldn't be hold by BC, meanwhile, dissociated ions were able to enter millipore of BC and competed sorption sites with PCP [23]. Consequently, the sorption–desorption capability of PCP on BC decreased under basic circumstances, and the desorption hysteresis effect was weaker for higher pH values. It is worth noting that RC showed this phenomenon markedly. It might be due to RC's highest surface area and pore volume of all BCs.

True hysteresis is often referred to as "irreversible sorption" [29]. In order to obtain the value q_e^{irr}, we extrapolated the desorption data linearly to the Y axis. The Y intercept is the solid phase concentration of the irreversibly sorbed compartment (q_e^{irr}) [30]. The q_e^{irr} values of RC, FC, and SC in each sorption–desorption cycle are listed in Table 5. For the purpose of greater closeness to q_{max}^{irr} value, we took the q_e^{irr} value in cycle 2 and cycle 4 as the q_{max}^{irr} value for pH 9.0 and pH 7.0. Thus, the q_{max}^{irr} values of RC, FC, and SC were 11.10, 0.98, 3.21 mg/g and 17.39, 1.52, 5.22 mg/g for pH 9.0 and pH 7.0, respectively. Notably, it is demonstrated that the irreversible sorption capacity of PCP to BC might correlate well with the pH value and BC types.

Generally speaking, apparent sorption–desorption hysteresis may result from: (1) one or more of several different types of experimental artifacts; (2) the irreversible binding to specific sorption sites; (3) slow rates of desorption; and (4) the sorbing molecule entrapment [31]. In this study, since desorption and sorption experiments were carried out under the same conditions, we considered that sorption–desorption hysteresis caused by experimental artifacts was negligible.

It was proposed that the sorption–desorption hysteresis observed could contribute to the irreversible entrapment and/or slow rate of desorption of sorbed molecules within porous structures of condensed SOM (soil/sediment organic matter) domains [31–33]. For example, Braida et al. [34] pointed out that the most likely explanation for the hysteresis of benzene in the charcoal was the irreversible pore deformation by the sorbate. In addition, Pignatello and coworkers [29,34] presented a "conditioning effect" theory which had been used in support of a pore deformation mechanism, which occurred by sorbate-induced alteration of the sorbent away from its thermodynamic state through an increase in the unrelaxed free volume.

The pore-deformation mechanism has been hypothesized as the main cause of the irreversible sorption of organic compounds to macromolecular NOM (natural organic matter), and considerable evidences have been published in support of this postulate [35–37]. From afore-mentioned data shown in Table 1, RC exhibited the highest surface area and porosity in these BCs. Simultaneously, we found that the irreversible sorption of RC in each cycle was mostly higher than that of SC or FC. Moreover, the negative ΔG^0 of each BC indicated that the sorption–desorption of BCs was not chemical but surface adsorption, therefore, we considered that the binding to surface functional groups of BC was not primary. In other words, the pore-deformation mechanism may be the main cause of the irreversible sorption of PCP to BCs.

The q_e^{irr}/q_e^{total} percentages of RC, FC, and SC were 65.5%, 68.1%, 44.0% at pH 9.0, and 76.8%, 78.4%, 53.4% at pH 7.0, respectively. The same trend was shown in the value of H. The pore structure of RC (Table 1) was the best, and RC's irreversible capacity was apparently the highest among all BCs tested; the pore structure of SC was between RC and FC, and the irreversible capacity was also higher than FC. Nonetheless, FC showed the most noticeable hysteresis effect. Due to the complex nature of this phenomenon, further studies using integrated technologies such as FTIR and carbon nuclear magnetic resonance (CNMR) spectroscopy, will still need to be carried out after sorption–desorption completed to clarify the true mechanisms of the sorption–desorption hysteresis.

Table 5
The value of q_e^{irr} for RC, FC, SC in each sorption–desorption cycle.

BC	Cycle 1		Cycle 2		Cycle 3		Cycle 4	
	q_e^{irr} (mg/g)	q_e^{irr}/q_e^{total} (%)	q_e^{irr} (mg/g)	q_e^{irr}/q_e^{total} (%)	q_e^{irr} (mg/g)	q_e^{irr}/q_e^{total} (%)	q_e^{irr} (mg/g)	q_e^{irr}/q_e^{total} (%)
RC	8.79 ± 0.69	58.5	11.10 ± 0.60	65.5	16.90 ± 0.40	79.9	17.39 ± 0.45	76.8
FC	0.80 ± 0.04	63.5	0.98 ± 0.06	68.1	1.26 ± 0.03	75.9	1.52 ± 0.05	78.4
SC	2.57 ± 0.43	41.7	3.21 ± 0.40	44.0	4.67 ± 0.26	52.1	5.22 ± 0.34	53.4

q_e^{irr}: the irreversible sorption capacity; q_e^{total}: the total sorption capacity.

4. Conclusions

Our experimental results showed that the measured PCP sorption capacity and the sorption–desorption hysteresis of BCs from three different origins were significantly influenced by the surface characteristics of BCs and the available form of PCP under different pH values. The obtained high sorption capacity of BCs, especially RC, may provide support for the concept of alternative endpoints for specific soil/sediment remediation in situ. The hysteresis phenomena observed here proved the potential impact of BCs on sequestration of HOCs in natural systems containing BC, and could offer some theoretical guidance for evaluating probability based on using BC to reduce the ecological risk of HOCs. However, it is recommended that future work with more advanced techniques will be applied to find the true main reasons behind the high sorption capacity and sorption–desorption hysteresis of HOCs sorption on BC, where the BC origin and the parameters characterizing the solution properties, such as the surface area, the pore volume, the functional groups of BC and the pH value, can be easily manipulated, to derive models applicable to a broader range of parameter values.

Acknowledgements

The work is financially supported by the grant from National Natural Science Foundation of China (no. 40801198), Zhejiang Provincial Major Science and Technology Special Projects (no. 2007C13060), Zhejiang Provincial Natural Science Foundation of China (no. R5090033).

References

[1] Y. Chun, G.Y. Sheng, C.T. Chiou, B.S. Xing, Compositions and sorptive properties of crop residue-derived, Environ. Sci. Technol. 38 (2004) 4649–4655.
[2] S. Kwon, J.J. Pignatello, Effect of natural organic substances on the surface and adsorptive properties of environmental black carbon (char): pseudo pore blockage by model lipid components and its implications for N_2-probed surface properties of natural sorbents, Environ. Sci. Technol. 39 (2005) 7932–7939.
[3] D. Werner, H.K. Karapanagioti, Comment on "modeling maximum adsorption capacities of soot and soot-like materials for PAHs and PCBs", Environ. Sci. Technol. 39 (2005) 381–382.
[4] R.M. Burgess, S.A. Ryba, M.G. Cantwell, J.L. Gundersen, R. Tien, M.M. Perron, Interaction of planar and nonplanar organic contaminants with coal fly ash: effects of polar and nonpolar solvent solutions, Environ. Sci. Technol. 25 (2006) 2028–2037.
[5] H.W. Sun, Z.L. Zhou, Impacts of charcoal characteristics on sorption of polycyclic aromatic hydrocarbons, Chemosphere 71 (2008) 2113–2120.
[6] T.D. Bucheli, Ö. Gustaffson, Quantification of the soot-water distribution coefficient of PAHs provides mechanistic basis for enhanced sorption observations, Environ. Sci. Technol. 34 (2000) 5144–5151.
[7] G. Cornelissen, Z. Kukulsaka, S. Kalaitzidis, K. Christanis, O. Gustafsson, Relations between environmental black carbon sorption and geochemical sorbent characteristics, Environ. Sci. Technol. 38 (2004) 3632–3640.
[8] G. Cornelissen, M. Elmquist, I. Groth, Ö. Gustaffson, Effect of sorbate planarity on environmental black carbon sorption, Environ. Sci. Technol 38 (2004) 3574–3580.
[9] Y. He, J.M. Xu, H.Z. Wang, Z.H. Ma, J.Q. Chen, Detailed sorption isotherms of pentachlorophenol on soils and its correlation with soil properties, Environ. Res. 101 (2006) 362–372.
[10] P.R. Haberston, J.A. Brandes, Y. Gelinas, A.F. Dicken, S. Wirick, G. Cody, Chemical composition of the graphitic black carbon fraction in riverine and marine sediments at sub-micron scales using carbon X-ray spectromicroscopy, Geochim. Cosmochim. Acta 70 (2006) 1483–1494.
[11] R.J. Li, B. Wen, S.Z. Zhang, Z.G. Pei, X.Q. Shan, Influence of organic amendments on the sorption of pentachlorophenol on soils, J. Environ. Sci. 21 (2009) 474–480.
[12] Y.N. Yang, G.Y. Sheng, Enhanced pesticide sorption by soils containing particulate matter from crop residue burns, Environ. Sci. Technol. 37 (2003) 3635–3639.
[13] M.T.O. Jonker, A.A. Koelmans, Sorption of polycyclic aromatic hydrocarbons and polychlorinated biphenyls to soot and soot-like materials in the aqueous environment mechanistic considerations, Environ. Sci. Technol. 36 (2000) 3725–3734.
[14] T.H. Nguyen, W.P. Ball, Absorption and adsorption of hydrophobic organic contaminants to diesel and hexane soot, Environ. Sci. Technol. 40 (2006) 2958–2964.
[15] V. Bindhumol, K.C. Chitra, P.P. Mathur, Bisphenol A induces reactive oxygen species generation in the liver of male rats, Toxicology 188 (2003) 117–124.
[16] Z.H. Duan, L. Zhu, L.Y. Zhu, Individual and joint toxic effects of pentachlorophenol and bisphenol A on the development of zebrafish (*Danio rerio*) embryo, Ecotoxicol. Environ. Saf. 81 (2008) 774–780.
[17] E.L.K. Mui, W.H. Cheung, G. McKay, Tyre char preparation from waste tyre rubber for dye removal from effluents, J. Hazard. Mater. 175 (2010) 151–158.
[18] Y.X. Chen, H.L. Chen, Y.T. Xu, M.W. Shen, Irreversible sorption of pentachlorophenol to sediments: experimental observations, Environ. Int. 30 (2004) 31–37.
[19] W.L. Huang, P.A. Peng, Z.Q. Yu, Effects of organic matter heterogeneity on sorption and desorption of organic contaminants by soils and sediments, Appl. Geochem. 18 (2003) 955–972.
[20] G. Cornelissen, Ö. Gustaffson, T.D. Bucheli, Extensive sorption of organic compounds to black carbon, coal and kerogen in sediments and soils: mechanisms and consequences for distribution, bioaccumulation and biodegradation, Environ. Sci. Technol. 39 (2005) 6881–6895.
[21] Y.P. Qiu, H.Y. Cheng, C. Xu, G.D. Sheng, Surface characteristics of crop-residue-derived black carbon and lead (II) adsorption, Water Res. 42 (2008) 567–574.
[22] L.C. Bornemann, R.S. Kookana, G. Welp, Differential sorption behaviour of aromatic hydrocarbons on charcoals prepared at different temperatures from grass and wood, Chemosphere 67 (2007) 1033–1042.
[23] Y. Yang, Y. Chun, G. Sheng, M. Huang, pH-Dependence of pesticide adsorption by wheat-residue-derived black carbon, Langmuir 20 (2004) 6736–6741.
[24] Y Shimizu, S. Yamazaki, Y. Terashima, Sorption of anionic pentachlorophenol (PCP) in aquatic environments: the effect of pH, Water Sci. Technol. 25 (1992) 41–48.
[25] M.G. Stapleton, D.L. Sparks, S.K. Dentel, Sorption of pentachlorphenol to HDTMA-clay as a function of ionic strength and pH, Environ. Sci. Technol. 28 (1994) 2330–2335.
[26] P.E. Diaz-Flores, R. Leyva-Ramos, R.M. Guerrero-Coronado, Adsorption of pentachlorophenol from aqueous solution onto activated carbon fiber, Ind. Eng. Chem. Res. 45 (2006) 330–336.
[27] X.Y. Yu, G.G. Ying, A.R.S. Kookana, Sorption and desorption behaviors of diuron in soils amended with charcoal, J. Agric. Food. Chem. 54 (2006) 8545–8550.
[28] M. Sanchez-Camazano, M.J. Sanchez-Martin, M.S. Rodriguez-Cruz, Sodium dodecyl sulphate-enhanced desorption of atrazine: effect of surfactant concentration and of organic matter content of soils, Chemosphere 41 (2000) 1301–1305.
[29] Y. Lu, J.J. Pignatello, Demonstration of the "conditioning effect" in soil organic matter in support of a pore deformation mechanism for sorption hysteresis, Environ. Sci. Technol. 36 (2002) 4553–4561.
[30] A.T. Kan, G.M. Fu, M.A. Hunter, M.B. Tomson, Irreversible adsorption of naphthalene and tetrachlorobiphenyl to Lula and Surrogate sediments, Environ. Sci. Technol. 31 (1997) 2176–2185.
[31] W.J. Weber Jr., W.L. Huang, H. Yu, Hysteresis in the sorption and desorption of hydrophobic organic contaminants by soils and sediments 2. Effects of soil organic matter heterogeneity, J. Contam. Hydrol. 31 (1998) 149–165.
[32] E.J. LeBoeuf, W.J. Weber Jr., A distributed reactivity model for sorption by soils and sediments: 8. Sorbent organic domains: discovery of a humic acid glass transition and an argument for a polymer-based model, Environ. Sci. Technol. 31 (1997) 1687–1702.
[33] B. Xing, J.J. Pignatello, B. Gigliotti, Competitive sorption between atrazine and other organic compounds in soils and model sorbents, Environ. Sci. Technol. 30 (1996) 2432–2440.

[34] W.J. Braida, J.J. Pignatello, Y.F. Lu, P.I. Ravikovitch, A.V. Neimark, B.S. Xing, Sorption hysteresis of benzene in charcoal particles, Environ. Sci. Technol. 37 (2003) 409–417.
[35] Y. Lu, J.J. Pignatello, History-dependent sorption in humic acids and a lignite in the context of a polymer model for natural organic matter, Environ. Sci. Technol. 38 (2004) 5853–5862.
[36] M. Sander, J.J. Pignatello, An isotope exchange technique to assess mechanisms of sorption hysteresis applied to naphthalene in kerogenous organic matter, Environ. Sci. Technol. 39 (2005) 7476–7484.
[37] T.H. Nguyen, H.H. Cho, D.L. Poster, W.P. Ball, Evidence for a pore-filling mechanism in the adsorption of aromatic hydrocarbons to a natural wood char, Environ. Sci. Technol. 41 (2007) 1212–1217.